Extending the Iron Energy Spectrum Measurements of the Cosmic Ray Isotope Spectrometer throughout 1997–2011

A. W. LABRADOR[1], R. A. MEWALDT[1], W. R. BINNS[2], E. R. CHRISTIAN[3], A. C. CUMMINGS[1], A. J. DAVIS[1], G. A. DE NOLFO[3], M. H. ISRAEL[2], R. A. LESKE[1], E. C. STONE[1], T. T. VON ROSENVINGE[3], M. E. WIEDENBECK[4]
[1]*California Institute of Technology, Pasadena, CA 91125 USA*
[2]*Washington University, St. Louis, MO 63130 USA*
[3]*NASA/Goddard Space Flight Center, Greenbelt, MD 20771 USA*
[4]*Jet Propulsion Laboratory, Pasadena, CA 91109 USA*
labrador@srl.caltech.edu
DOI: 10.7529/ICRC2011/V06/0791

Abstract: The Cosmic Ray Isotope Spectrometer (CRIS) aboard the Advanced Composition Explorer has been measuring galactic cosmic ray elemental and isotopic abundances of boron through nickel since late 1997. The CRIS instrument itself is a silicon detector telescope stack using eight energy deposit measurements to identify particles and their energies using a ΔE vs. E' measurement technique, with particles stopping in one of the detector layers. In this paper, we make preliminary measurements for particles penetrating through the bottom of the detector stack, extending energy measurements above 700 MeV/nuc for iron, and we examine these extended energies throughout the available data from 1997 to 2011. During this period, CRIS observed iron minimum and maximum intensities in 2000 and 2009, respectively, with the maximum intensities setting the record as the highest intensities of the space era to date.

Keywords: Cosmic rays; elements.

1 Introduction

The Cosmic Ray Isotope Spectrometer (CRIS) aboard the Advanced Composition Explorer (ACE) has been measuring galactic cosmic ray abundances since late 1997, minus days of significant solar activity [1]. The ACE flight has allowed CRIS to measure spectra from boron to nickel through an entire solar cycle, spanning both solar minimum and solar maximum [2]. In 2009, the measured iron intensities set a record maximum for the space era [3].

The CRIS instrument is a silicon detector telescope providing up to nine energy deposit measurements for particles entering the detector stack. Particle trajectories are measured by a scintillating optical fiber trajectory (SOFT) system. Charged particles are identified by ΔE vs. E' measuring technique, with results for particles stopping in the stack available to the public at the ACE Science Center on the World Wide Web [4].

We have previously described a technique to identify charged particles that penetrate through the bottom of the instrument, which allows measurements at energies higher than for those particles that stop in one of the detectors [5]. That technique is computationally intensive, and in this paper, we describe a simpler approach that we apply more quickly to the entire flight. We show that the penetrating iron intensity measurements above 528 MeV/nuc parallel the behavior of the lower energy, stopping iron.

2 Penetrating Iron Selection

Figure 1 shows a sample of CRIS penetrating data, displayed as ΔE vs. E', where ΔE is the sum of the measured ionization energy deposits, in MeV, for a given particle in the top four detectors (named E1-E4) in the CRIS silicon detector stack, and E' is the sum of the measured ionization energy deposits in the next four detectors (E5-E8). An angle of incidence correction is also applied to the data. A ninth detector (E9) does not provide direct energy deposit measurement in this analysis; a positive signal in E9 indicates a particle that penetrates through the top eight detectors, while no signal in E9 indicates a particle that stops in E8 or earlier in the stack. A particle that stops in E1 through E8 is assigned a range number

(RNG) corresponding to its stopping detector, while a particle that yields a signal in E9 is said to be penetrating (PEN).

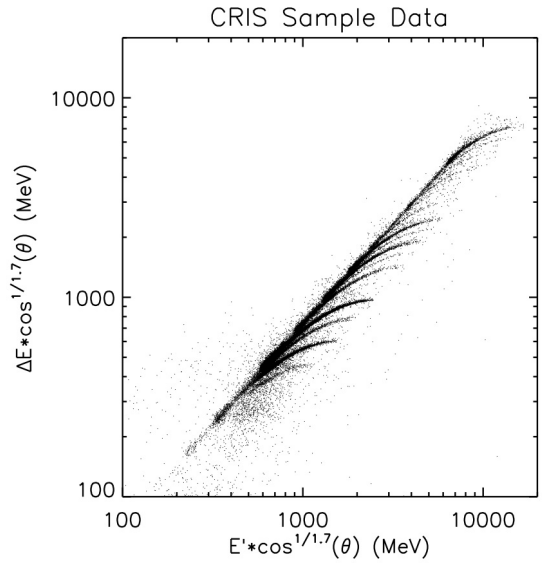

Figure 1. Sample CRIS measurements for penetrating particles, showing elements from B, C, N, and O through Fe.

The particles in Figure 1 are those that show a positive E9 signal and are penetrating. Signals from B, C, N, and O are at the bottom of the figure, while higher charge particles like Fe are at the top. In the figure, higher energy particles on the figure follow the right-pointing tracks down and to the left with increasing energy, tracing the decreasing ionization energy loss of the Bethe-Bloch equation with increasing incident energy. At even higher energy, where the Bethe-Bloch equation shows a relativistic rise in ionization energy loss, there is a fold-back up and to the right in the figure, not visible at this scale.

Figure 2 shows a close-up of the same CRIS pulse height data, focusing on the iron particles. Previous penetrating particle analysis attempted to identify particles by charge, mass, and energy by making fits of the pulse height signals to range-energy curves [5]. For this analysis, Fe particles are simply selected from regions in ΔE vs. E' space.

In Figure 2, the dashed lines set boundaries for minimum ionizing particles, not only for Fe but for all of the elements detected by CRIS. Region 1 is bounded on top and bottom to exclude the expected average signals of Co and Mn (bracketing Fe on the top and bottom). Signals in Region 1 are selected for Z=26±0.5. Region 1 is also bounded on the left by the minimum ionizing region, and on the right by the energies needed to penetrate just to the bottom of E8. We take the Fe RNG8 upper energy boundary of 471 MeV/nuc as the lower energy boundary of Region 1. The upper Fe energy boundary is approximately 746 MeV/nuc in region 1, at the average angle of incidence for particles in this analysis. Thus, the approximate energy range for Region 1 is 471–746 MeV/nuc. Three energy bins within Region 1 are selected for this analysis: 528–603 MeV/nuc, 603–675 MeV/nuc, and 675–746 MeV/nuc. These energy bins are preliminary and approximate, as is the total energy range for Region 1. They are calculated from the same range-energy curves calculated for our older analysis [5], and they are set for the average angle of incidence of the particle events included in this analysis. The distribution of actual angles of incidence in the data set results in overlap between the energy ranges.

Region 2, as shown, then corresponds to all penetrating Fe particles with energies of approximately 746 MeV/nuc and higher, including Fe at minimum ionizing energies and beyond.

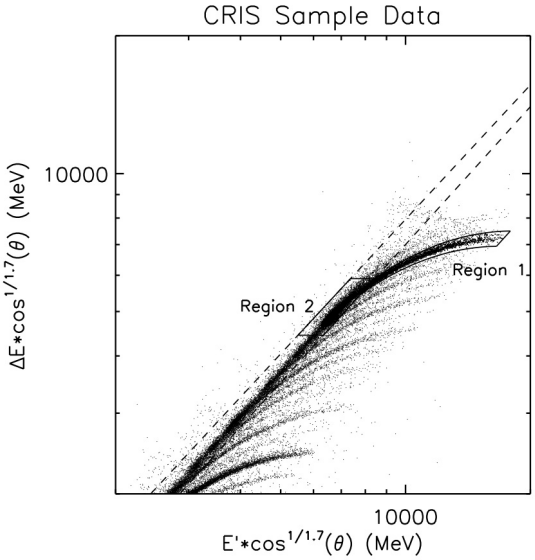

Figure 2. Sample CRIS measurements for penetrating particles, showing selection regions for penetrating Fe used in this analysis.

It must be noted that, although previous methods for penetrating particle analysis attempted to identify individual particles by element, selection of particles by ΔE vs. E' in this analysis does not attempt to identify individual particles, only their approximate charge and energy. Region 1, for example, must be set large enough to select as much Fe as possible, but it may also accept some fraction of nearby, less abundant elements such as Mn and Co as background.

3 Analysis

In order to calculate intensities, particle counts for a given species and energy are divided by geometry factor, livetime, and energy bin width, and corrections are made for spallation losses and SOFT hodoscope efficiency. We remove from this analysis those days when the CRIS instrument is inactive, as flagged by the CRIS level 2

data from the ACE Science Center [4]. Minimum and maximum intensities are seen in 2000 and 2009, respectively, in that data. For this analysis, we approximate the geometry factor, spallation losses, and SOFT hodoscope efficiency for penetrating particles with the same values as we use for the RNG8 stopping particles.

For penetrating particles, additional care must be taken. While data from particles that stop in the instrument are telemetered at high priority, penetrating particle data are telemetered at lower priority. Lower priority particles like penetrating particles are all counted by the CRIS instrument, but only a fraction of those events are telemetered as pulse height events for detailed analysis. This detailed analysis includes penetrating particle selection and identification by element. Therefore, penetrating particle intensities must be corrected to account for that telemetry fraction.

Furthermore, as noted in the previous section, the Fe particle selection method is clearly susceptible to background contamination from nearby elements like Mn and Co, arising from fluctuations in individual energy deposit measurements. A more thorough analysis to remove or reduce background contribution would involve attempts to identify individual particles by energy deposit using methods associated with the earlier analysis [5] or by examining the collective ΔE and E' measurements slices and attempting to fit identifiable peaks of Mn, Fe, and Co. We intend to complete such analysis by the time of the conference and for a possible revised paper.

For this preliminary analysis, we instead examine ACE/CRIS level 2 data for Mn, Fe, Co, and Ni at RNG 8, from the ACE Science Center. From the element count data, the number of Mn and Co counts in CRIS data, combined, are ~10% as high as the CRIS Fe counts. With Ni added, the counts are ~15% as high as the Fe counts. Since the Region 1 boundaries are theoretically set to exclude the Mn and Co track centers in Figure 2, we may assume that less than half of the Mn and Co counts in the data are counted as Fe from Region 1. Therefore, we can estimate a hard upper limit of no more than 5% (and probably significantly less) of the penetrating Fe counts in Region 1 are background contamination from Mn and Co. This fraction should be approximately constant over the solar cycle.

Region 2 will experience even more cross-contamination between Fe and other elements. For this region, we make a preliminary estimate that as many as 15% of the Region 2 Fe counts may be Mn, Co, and Ni contamination, as well as contamination from other, nearby elements.

Figures 3 shows 27 day (Bartels Rotation) average Fe intensities vs. time for the ACE flight. In the top panel are the RNG8 Fe intensities (431-471 MeV/nuc), reproducing the level 2 data available from the ACE Science Center. The three PEN Fe Region 1 (528–746 MeV/nuc) intensities vs. time are shown combined into one energy bin in the middle panel. The PEN Fe Region 2 (>746 MeV/nuc) integrated intensity vs. time is shown in the bottom panel.

As seen in Figure 3, the CRIS Fe intensities reached minimum in 2000 and maximum in 2009 (or solar maximum and solar minimum, respectively). We see that the intensity in 2009 exceeds that during the 1997-1998 solar minimum, as observed at lower energy [3]. The amount by which the 2009 intensities exceed those of the 1997-1998 solar minimum will be determined following more detailed analysis. The general behavior observed in RNG8 is repeated in the three energy bins in Region 1 and somewhat in Region 2, though the effect of solar modulation at higher energies is reduced.

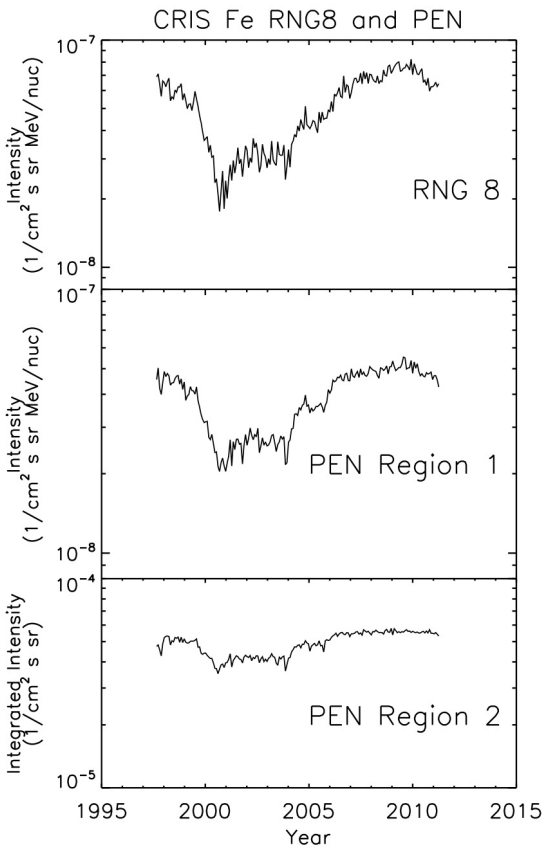

Figure 3. 27 day (Bartels Rotation) average Fe intensities vs. time for CRIS in RNG8 (431-471 MeV/nuc) and PEN Region 1 (528-746 MeV/nuc). Also shown are 27 day average Fe integrated intensities for PEN Region 2 (>746 MeV/nuc). Note that the PEN intensities in 2009 are greater than those in the 1997-1998 solar minimum.

4 Results and Further Analysis

Figure 4 shows three spectra: One from days 226-306 of 1997 (solar minimum, Bartels Rotations 2240-2242), one from days 238-318 of 2000 (solar maximum, Bartels Rotations 2281-2283), and one from day 298 of 2009

through day 13 of 2010 (solar minimum, Bartels Rotations 2405-2407). The open diamonds are the ACE/CRIS level 2 data available from the ACE Science Center, and the open squares are the preliminary PEN Region 1 measurements from this analysis. Uncertainties are statistical.

Overlaid onto Figure 4 are curves representing a model Fe spectrum solar modulated to the solar minimum and solar maximum intensity levels shown by the data. The curves are fit to the data by taking a model Fe spectrum for the interstellar medium, modulating the model spectrum in 25 MV modulation parameter intervals up to 1500 MV, and interpolating between the three best chisquare fits to improve the precision to within 1 MV. This model is the same as was used by [2], and the modulation calculation was a simple spherically symmetric calculation [6]. As was noted in the earlier paper, improved fits to the spectra at 1 AU may be obtained with more detailed solar modulation models, and such calculations may be the focus of future work

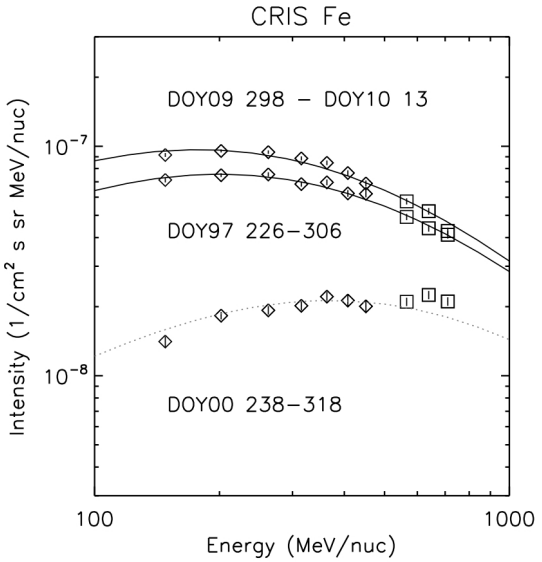

Figure 4. 81 day average Fe spectra from 1997, 2000 and 2009-2010. The open diamonds are ACE/CRIS level 2 data, and the open squares are the 528-746 MeV/nuc PEN Fe data from this analysis. Uncertainties are statistical.

Generally, we find that the behavior of the penetrating particle intensities follows the behavior expected from the solar modulated model spectra, with greater relative differences between solar minimum intensities near the Fe peak than at the higher energies. At penetrating energies, the 2009-2010 solar minimum Fe intensities exceeded those of the 1997 solar minimum by about 20%, compared to the ~26% increase at the lower energies.

Figure 4 still represents a preliminary analysis for penetrating Fe in CRIS data, with the selection of Region 1 penetrating Fe is still being examined. We find that the penetrating Fe counts that enter the intensity calculations are sensitive to the boundaries selected for Region 1, and in particular, the higher energy penetrating points may be suppressed by the narrowing of the Region 1 selection box as it approaches minimum ionizing. The selection region can be widened to accept significantly more particles, at the expense of accepting additional background. As this background from Mn and Co should not exceed approximately 5% of the total counts, this background may be acceptable. Additional continuous widening of the Region 1 box may be achieved by setting the cuts as a function of ΔE or E' rather than as a constant in Z.

This research is supported by NASA under Grants NNX08IA11G and NNX10AE45G.

5 References

[1] E.C. Stone et al., Space Science Reviews, 1998, **96**, 285-356.
[2] J.S. George et al., Astrophysical Journal, 2009, **698**, 1666-1681.
[3] R. A. Mewaldt et al., Astrophysical Journal Letters, 2010, **723**, 1-6.
[4] http://www.srl.caltech.edu/ACE/ASC/
[5] A. W. Labrador et al.: Proceedings of the 28th International Cosmic Ray Conference, 2003, **4**, 1773-1776.
[6] L. A. Fisk, J. Geophys. Res., 1971, **76**, 221.